MODELING OF EFFECTIVE HEAT TRANSFER PROPERTIES IN BASIC CELLS OF BINARY-COMPONENT PACKED BEDS

P. J. Turyk
Division of Mechanical Engineering
National Research Council of Canada
Ottawa, Ontario, Canada

M. M. Yovanovich
Division of Mechanical Engineering
University of Waterloo
Waterloo, Ontario, Canada

ABSTRACT

A simple model for the heat transfer in binary-component packed beds is presented. The model is a modification to the basic-cell approach previously developed. The interstitial spheres were arranged in a simple manner in the gap between the primary-component spheres. The sample calculations showed that at low values of the gas parameter M (high gas pressure), the interstitial spheres increased the total effective conductivity of the basic cell.

NOMENCLATURE

A	area (m^2)
a	contact radius (m)
D	sphere diameter (m)
D_a	diameter defined in Equation (19) (m)
D_d	diameter defined in Equation (17) (m)
E	Young's modulus (Pa)
I	integral terms defined in the text
k	thermal conductivity (W/m/K)
K	thermal conductivity ratio (k_o/k_s)
L	dimensionless diameter D/2a
ℓ	heat transfer length (m)
L_a	$=D_a/2a$
L_d	$=D_d/2a$
M	dimensionless gas parameter ($2\alpha\beta\Lambda/D$)
m	number of rings of interstitial spheres
N	mechanical load (N)
n	number of spheres in the interstitial stack
N_i	number of spheres in a ring of interstitial spheres
P	gas pressure (Pa)
Pr	Prandtl number
Q	heat flow (W)
r	radius coordinate (m)
R	thermal resistance (K/W)
r_c	radius of locus of interstitial sphere centres (m)
r_i	radius location defined in Equation (18) (m)
S_l	$=x_{ci}-L\epsilon_i$
S_u	$=x_{ci}+L\epsilon_i$
T	temperature (K)
x	dimensionless radius with respect to contact radius (r/a)
x_c	$=r_c/a$
x_i	$=r_i/a$

Greek symbols

α	accommodation coefficient
β	thermophysical gas property ($2\gamma/Pr/(\gamma+1)$)
γ	specific heat ratio
δ	dimensionless gap width with respect to contact radius
ϵ	sphere size ratio D_{small}/D_{large}
θ	function defined by Equation (35)
θ	angular coordinate (deg)
Λ	gas mean free path (m)
ν	Poisson coefficient

Subscripts and Superscripts

1	secondary phase; gas alone; plane 1
12	between planes 1 and 2
2	with interstitial spheres; plane 2
c	contact
g	gas
ge	gap effective
ht	heat transfer
Hz	Hertzian, to denote gap width between primary spheres
i	ring index
o	reference conditions; continuum
s	solid
t	total
te	total effective
′	for a single stack of interstitial spheres
*	dimensionless with respect to k_o

INTRODUCTION

Heat transfer in packed beds has been extensively studied for a wide variety of applications: fluidized-bed reactors and combustors, grain driers, soils and solar thermal-energy rock beds, insulation, powders, ceramics, and pebble-bed nuclear reactors. In each case, there is a need to know the geometric and mechanical characteristics of the beds, and the heat transport within the beds.

This paper describes an initial attempt at modelling the geometry and heat transfer within a binary-component packed bed of spheres. In a binary-component packed bed, a secondary phase of small spheres fills the interstices formed by the matrix of large spheres. The formulation proceeds with the development of a simple model for the structure of the spheres which fill the interstitial space between the large primary-component spheres of the bed, followed by the heat transfer analysis. The result will be an expression for the effective thermal conductivity of the cell, and some parametric calculations will be presented.

The analysis of the heat transfer properties in binary-component beds presented here was originally intended for the determination of effective conductivity of unrestructured sphere-pac fuel used in some types of power generating nuclear reactors (Turyk, 1985). Peterson, Fletcher and Peddicord (1987) reviewed various experimental and analytical research in this area. They concluded that the heat transfer mechanisms in multicomponent packed beds are not clearly understood, and that additional analytical work is required.

The geometry and heat transfer analysis is performed for a unit of the packed bed called the basic cell. This type of analysis isolates a single element of the packed bed, and examines the heat transfer mechanisms within it, with the intent of applying the results to the rest of the bed. The basic cell is an idealization of the structure of the packed bed. It assumes that the bed is infinite, i.e., no boundary effects, and regularly packed throughout; the basic cell in this formulation corresponds to the simple cubic packed arrangement. However ideal, the results of the analysis in this approach can be used in higher order forms of packed bed heat transfer analysis, such as the Monte Carlo approach of Yang, et al. (1982). Thus, the results of the basic-cell analysis can provide valuable insight into the mechanisms of heat transfer within the entire bed.

The basic-cell approach for the binary-component packed bed was chosen to build upon the previous formulations of Yovanovich (1967), Kitscha and Yovanovich (1975), and Ogniewicz and Yovanovich (1978). The following assumptions and arrangements are used in the development of the model:

- the primary component bears a mechanical load N;
- the secondary component bears no load (point contact), including the primary-secondary interface;
- the secondary component is packed in the simple orderly fashion shown in Figure 4;
- a gas fills the interstitial gap;
- the interstitial gas is quiescent: no natural or convective heat transfer;
- radiation heat transfer is neglected, but is important if the temperature gradient is high;
- the secondary-component spheres are one-tenth the size of the primary component;
- one-dimensional heat transfer in the interstitial gap predominates (Figure 3);
- the midplanes of the primary spheres are isothermal; and
- the primary and secondary components share a common thermal conductivity k_s.

The text will proceed with a review of the underlying method developed by Yovanovich, Kitscha, and Ogniewicz, and then will present the modification required to account for the presence of the secondary components.

REVIEW OF BASIC THEORY

The basic method provides an expression for the dimensionless effective thermal conductivity of the system shown in Figure 1. A concise review of the basic-cell heat transfer method of Yovanovich (1967), Kitscha and Yovanovich (1975), and Ogniewicz and Yovanovich (1978) was presented in Turyk and Yovanovich (1985), and is summarized here.

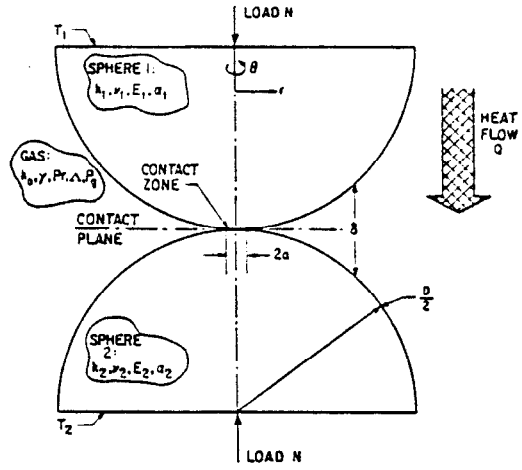

Figure 1 Simple Cubic Packing Basic Cell

In Figure 1, the mechanical load creates material deformation at contact, resulting in a finite contact area of radius a, given by

$$a^3 = \frac{3}{8} ND \frac{1-\nu^2}{E} \tag{1}$$

from Hertz elastic contact theory (Timoshenko and Goodier, 1970). For an imposed temperature differential of $\Delta T_{12}=T_1-T_2$, the heat flow across the cell is

$$Q_t = \frac{\Delta T_{12}}{R_t} \tag{2}$$

The total heat flow is composed of two elements, heat transfer through the contact spot and the interstitial gap, which are represented by the contact and gap resistances, respectively (Figure 2):

$$\frac{1}{R_t} = \frac{1}{R_c} + \frac{1}{R_g} \tag{3}$$

The contact resistance is given by

$$\frac{1}{R_c} = 2k_s a \tag{4}$$

The gap resistance is calculated from

$$Q_g = \frac{\Delta T_{12}}{R_g} \tag{5}$$

where

$$Q_g = \iint d^2Q_g = \iint_A \frac{k_g \Delta T}{\delta_{Hz}} d^2A \tag{6}$$

Each of the integrand parameters in Equation (6) are dependent on the location within the gap, which, assuming axisymmetry, is represented by the radius r, as follows:

The gas conductivity depends on the gap width and is given by

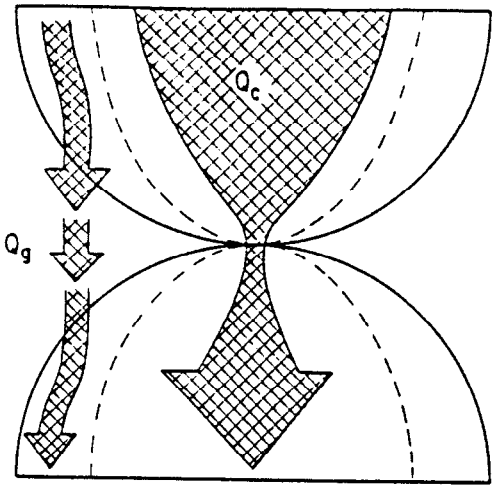

Figure 2 Heat Conduction in the Basic Cell

$$k_g(x) = \frac{k_o}{1 + \alpha\beta\Lambda/\delta_{Hz}} \tag{7}$$

where k_o is the continuum gas conductivity, α is the thermal accommodation coefficient between the spheres and the gas, β is a thermophysical property of the gas, and Λ is the mean free path of the gas. The mean free path varies with temperature and pressure according to

$$\Lambda = \Lambda_o \frac{T}{T_o}\cdot\frac{P_o}{P} \tag{7a}$$

where the subscript o indicates reference conditions. The gap width in dimensionless form is

$$\delta_{Hz}(x) = 2\left[\sqrt{L^2-1} - \sqrt{L^2-x^2} + \frac{1}{\pi L}\left((2-x^2)\sin^{-1}(1/x) + \sqrt{x^2-1} - \pi/2\right)\right] \tag{8}$$

where $L=D/2a$, and $x=r/a$. The temperature varies according to

$$\Delta T(x) = \Delta T_{12}(2/\pi)\tan^{-1}\sqrt{x^2-1} \tag{9}$$

With $d^2A=2\pi r dr$, and substituting equations (7) and (9) into (6), integrating from r=a to r=D/2, nondimensionalizing, and simplifying,

$$Q_g = 2k_o a\Delta T_{12}\int_1^L \frac{2x\tan^{-1}\sqrt{x^2-1}}{\delta_{Hz} + ML}\,dx \tag{10}$$

$$Q_g = 2k_o a\Delta T_{12} I \tag{10a}$$

in which I is integrated by adaptive numerical quadrature. The mechanical load is represented by the dimensionless sphere diameter, $L=D/2a$, which varies between L=50 and L=1000 for heavy and light loads, respectively. The gas parameter M varies directly with temperature, and inversely with pressure.

The gap resistance is

$$\frac{1}{R_g} = \frac{Q_g}{\Delta T_{12}} = 2k_o a I \tag{11}$$

and the total resistance is

$$\frac{1}{R_t} = 2k_o a\left[\frac{k_s}{k_o} + I\right] \tag{12}$$

The resistance is converted into a conductivity by

$$k_{te} = \frac{\ell}{R_t A_{ht}} \tag{13}$$

Taking $\ell=D$ and $A_{ht}=D^2$, the dimensionless effective thermal conductivity of the basic cell is

$$k_{te}^* = \frac{k_{te}}{k_o} = \frac{1}{L}\left[\frac{1}{K} + I\right] \tag{14}$$

which reduces the dependence of the conductivity to three parameters:

$$k_{te}^* = f(L,M,K) \tag{15}$$

The variation of conductivity k_{te}^* with these parameters will be described in the sample calculation section, in comparison with the effective conductivity of the binary cell.

BINARY-COMPONENT CELL

The assumptions presented in the problem statement concerning point contact for the secondary-component spheres and the one-dimensional heat flow within the gap (Figure 3) simplify the modification of the basic model for the binary phase:

- the contact conductance remains unchanged,
- the temperature distribution of the primary component remains unchanged, and
- the gap conductance is altered only in the regions occupied by the secondary component.

The modifications to the basic model are presented in this section starting with the examination of the geometry of the system, followed by the heat transfer analysis.

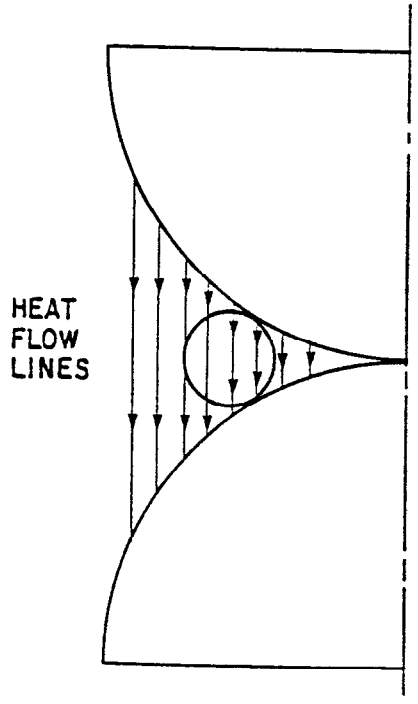

Figure 3 One-Dimensional Heat Flow

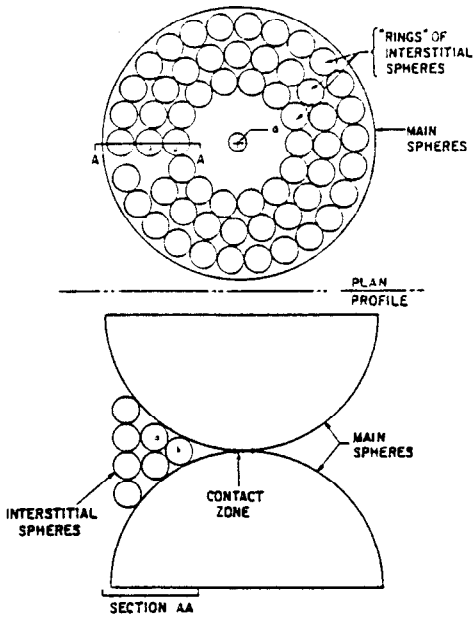

Figure 4 Simple Binary-Component Basic Cell

Geometry

The interstitial spheres are arranged in the simple manner shown in Figure 4. This is, of course, a highly idealized view of the packing of spheres in the gap between the spheres of the primary component. However, the mathematical analysis is simplified, and it is only a first step in analyzing the heat transfer in such a system.

Three parameters necessary to carry out the heat transfer analysis characterize the geometry of this system. They are: r_{ci}, the radial distance of the locus of centres of the interstitial spheres in the ith ring from the axis of symmetry of the primary components (Figures 5 and 6); N_i, the number of stacks of spheres in the ith ring; and $\delta_i(r,\theta)$, the gap between the primary-component sphere and the adjacent secondary-component sphere in the ith ring (Figure 5). These parameters are determined given the number of spheres in the ith stack, n_i.

From Figures 5 and 6, r_{ci} is given by

$$2r_{ci} = \left[(D_i+D_{di})^2 - (D_a-(n_i-1)D_i)^2\right]^{\frac{1}{2}} \tag{16}$$

where

$$\frac{D_{di}}{2} = \left[r_{ii}^2 + \left(\frac{D_d-\delta_{Hz}(r_i)}{2}\right)^2\right]^{\frac{1}{2}} \tag{17}$$

$$r_{ii} = \frac{r_{ci}D_{di}}{D_i + D_{di}} \tag{18}$$

$$\frac{D_d}{2} = \left[(D/2)^2-a^2\right]^{\frac{1}{2}} - \frac{a^2}{D} \tag{19}$$

The various methods of describing the primary sphere diameter (D, D_a, and D_d) are necessary because of the deformation of the surfaces under load. This is accounted for by the appearance of the terms δ_{Hz} and a in the equations. Equations (16) to (19) are nondimensionalized as follows:

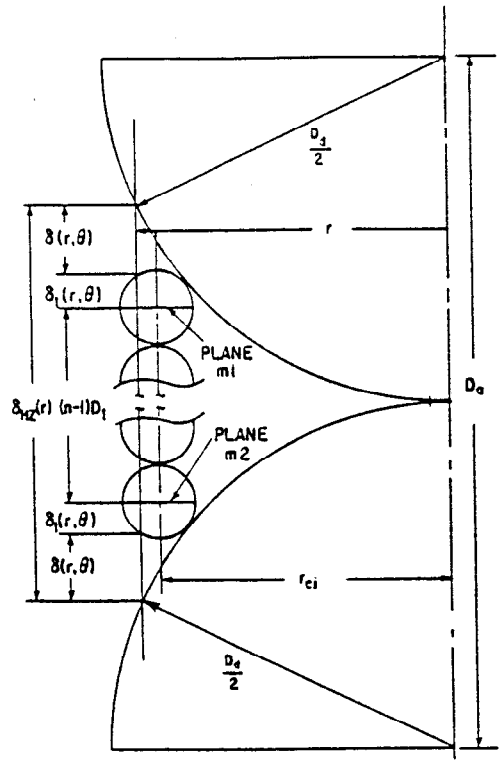

Figure 5 Geometry for Interstitial Spheres

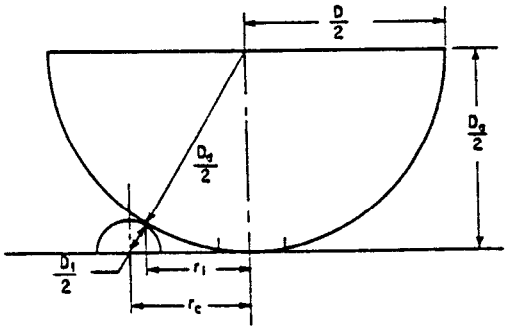

Figure 6 Definition of r_c

$$x_{ci} = \left[(L_{di}+L\epsilon_i)^2 - (L_a-(n_i-1)L\epsilon_i)^2\right]^{\frac{1}{2}} \tag{20}$$

$$L_{di} = \left[x_{ii}^2 + \left(L_a-\frac{\delta_{Hz}(x_{ii})}{2}\right)^2\right]^{\frac{1}{2}} \tag{21}$$

$$x_{ii} = \frac{x_{ci}L_{di}}{L\epsilon_i + L_{di}} \tag{22}$$

$$L_a = \sqrt{L^2-1} - \frac{1}{2L} \tag{23}$$

By calculating L_a, the simultaneous Equations (20) to (22) can be solved iteratively to yield x_{ci}.

The number of stacks in a ring, N_i, is calculated with the aid of Figure 7:

$$N_i = \text{int}\left(\frac{\pi}{\phi_{si}}\right) \tag{24}$$

where

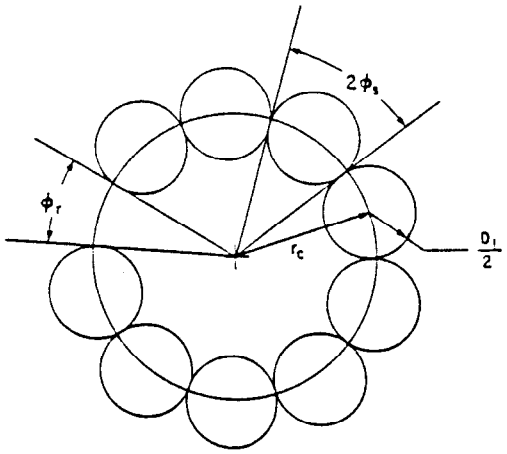

Figure 7 Spheres in Ring of Diameter r_c

$$\phi_{si} = \sin^{-1}\left(\frac{D_1}{2r_{ci}}\right) = \sin^{-1}\left(\frac{L\epsilon_1}{x_{ci}}\right) \qquad (25)$$

and int(·) denotes the integer operator (truncation of the fractional portion). The dependence of N_i on the number of spheres in the stack is carried by x_{ci}.

The gap width $\delta_1(r,\theta)$ is the distance between the main sphere and the adjacent interstitial sphere, shown in Figure 5. It is dependent on both the distance from the system centreline, r, and on the angular position, θ, shown in Figure 8 for n_i=1, and is given by the expression

$$2\delta_1(r,\theta) = \delta_{Hz}(r) - ((n_i-1)D_1 + 2\delta_{1i}(r,\theta)) \qquad (26)$$

where

$$\delta_{1i}(r,\theta) = \left[(D_1/2)^2 - r_{1i}^2\right]^{\frac{1}{2}} \qquad (27)$$

is the distance from the midplane (plane m1 or m2 in Figure 5) of the interstitial sphere to its surface. The local coordinate r_1 is shown in Figure 9, and is converted from the global coordinate system by

$$r_{1i}^2 = r_{ci}^2 + r^2 - 2rr_{ci}\cos\theta \qquad (28)$$

Equations (26) to (28) are nondimensionalized to

$$2\delta_1(x,\theta) = \delta_{Hz}(x) - ((n_i-1)L\epsilon_1 + 2\delta_{1i}(x,\theta)) \qquad (29)$$

$$\delta_{1i}(x,\theta) = \sqrt{(L\epsilon_1)^2 - x_{1i}^2} \qquad (30)$$

and

$$x_{1i}^2 = x_{ci}^2 + x^2 - 2xx_{ci}\cos\theta \qquad (31)$$

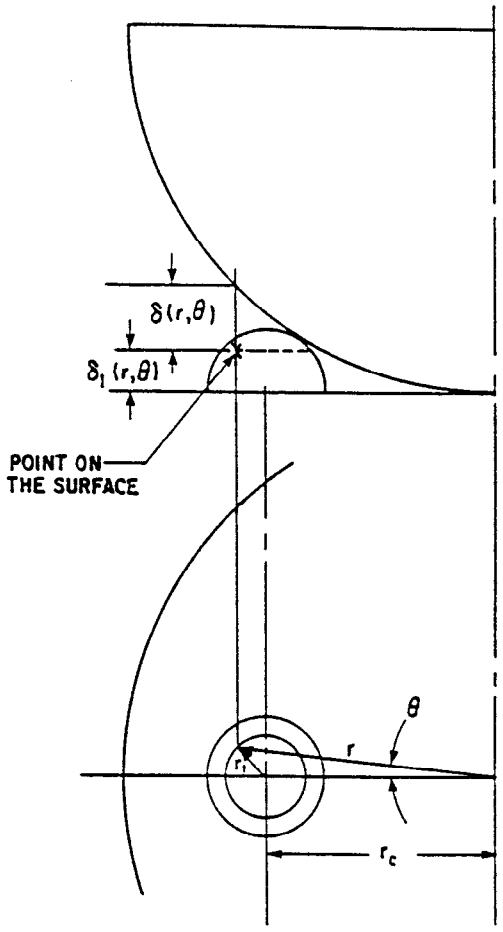

Figure 8 Definition of Gap Width δ

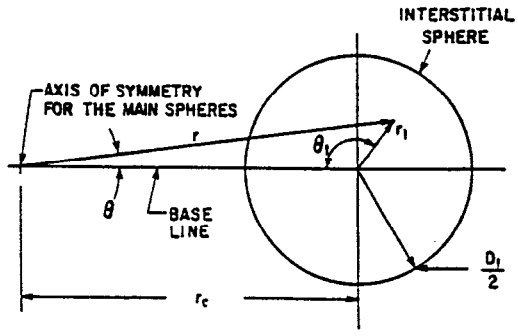

Figure 9 Local and Global Coordinate Systems

Heat Transfer

Enough geometric information is now available to calculate the heat transfer in a stack of interstitial spheres, Figure 10. The approach taken to modify the gap conductance is:

1) subtraction of the contribution to the gap conductance in this region by the gas alone, followed by

2) addition of the contribution to the conductance by the stacks of interstitial spheres in this region.

This is allowable given the assumptions for this system, as explained at the beginning of this section.

To subtract the gas-alone contribution, the local heat transfer must be formulated as in the basic model. Equation (6) is recast as

$$d^2Q_g = \frac{k_g\Delta T}{\delta_{Hz}} r d\theta dr \qquad (32)$$

which must be integrated over the region of influence, i.e. the region occupied by the stack of interstitial spheres.

The limits of integration on r are:

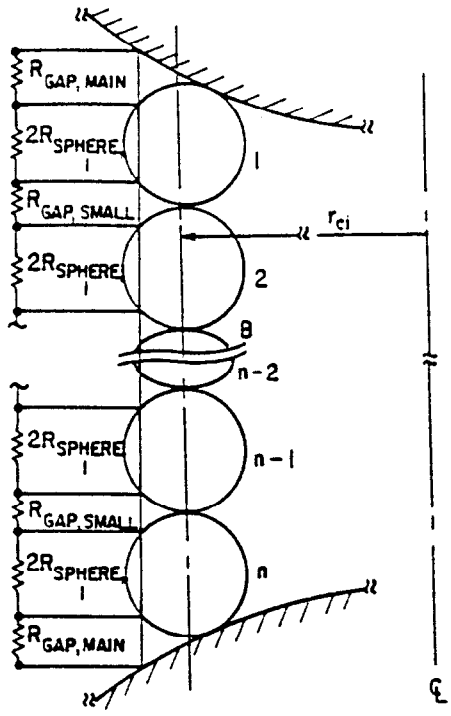

Figure 10 Heat Transfer Through Interstitial Spheres

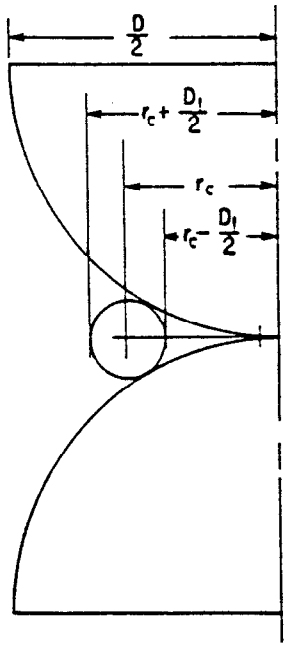

Figure 11 Radial Limits of Integration

$$r_{ci} - \frac{D_1}{2} \le r \le r_{ci} + \frac{D_1}{2} \tag{33}$$

as shown in Figure 11. The limits of integration on θ are

$$0 \le \theta \le \theta_1 \tag{34}$$

where θ_1 is obtained by substituting $r_1=D_1/2$ into Equation (28), and isolating θ:

$$\theta_1(r) = \cos^{-1}\left[\frac{r^2 + r_{ci}^2 - (D_1/2)^2}{2rr_{ci}}\right] \tag{35}$$

Substituting Equations (7) and (9) into Equation (32), nondimensionalizing, integrating, and simplifying gives

$$Q_{g1i} = \frac{2k_a a\Delta T_{12}}{\pi} \int_{S_L}^{S_U} \int_{0}^{\theta_1} \frac{x\tan^{-1}\sqrt{x^2-1}}{\delta_{Hz} + ML} \, d\theta dx \tag{36}$$

where

$$S_U = x_{ci} + L\epsilon_1 \tag{36a}$$

$$S_L = x_{ci} - L\epsilon_1 \tag{36b}$$

The subscript 1 denotes heat transfer for the gas alone, from the basic-cell formulation. The integrand of Equation (36) is not dependent on θ, so that

$$Q_{g1i} = \frac{2k_a a\Delta T_{12}}{\pi} \int_{S_L}^{S_U} \frac{\theta_1 x\tan^{-1}\sqrt{x^2-1}}{\delta_{Hz} + ML} \, dx \tag{37}$$

where

$$\theta_1 = \cos^{-1}\left[\frac{x^2 + x_{ci}^2 - (L\epsilon_1)^2}{2xx_{ci}}\right] \tag{37a}$$

The resistance of this component is

$$\frac{1}{R_{g1i}} = \frac{Q_{g1i}}{\Delta T_{12}} = \frac{2k_a a}{\pi} \int_{S_L}^{S_U} \frac{\theta_1 x\tan^{-1}\sqrt{x^2-1}}{\delta_{Hz} + ML} \, dx \tag{38}$$

$$\frac{1}{R_{g1i}} = \frac{2k_a a}{\pi} I_{g1i} \tag{38a}$$

I_{g1i} is evaluated by adaptive numerical quadrature. There are $2N_i$ of these regions in the ith ring of interstitial spheres. The resistances are added in parallel to give

$$\frac{1}{R_{g1i}} = 2k_a a \left[\frac{2N_i}{\pi} I_{g1i}\right] \tag{39}$$

To calculate the contribution of the interstitial spheres to the gap conductance, the resistances of the various components in the heat flow path between the primary spheres are added in series, as shown in Figure 10. The local heat flow expression is

$$d^2Q_{g2i} = \frac{\Delta T}{\sum R} = \frac{\Delta T}{2R_{gap,main} + 2n_i R_{sphere,1} + (n_i-1)R_{gap,small}} \tag{40}$$

where

$$R_{gap,main} = \frac{\delta_1(r,\theta)}{k_g d^2 A} \tag{41}$$

$$R_{sphere,1} = \frac{\delta_{s,1}(r,\theta)}{k_s d^2 A} \tag{42}$$

and

$$R_{gap,small} = \frac{D_c - 2\delta_{i1}(r,\theta)}{k_g d^2 A} \tag{43}$$

The subscript 2 refers to heat transfer with interstitial spheres present. Substituting Equations (41) to (43) into (40), as well as Equations (7), (9), and (26) for k_g, ΔT, and δ_i, nondimensionalizing and simplifying results in

$$d^2Q_{g2i} = \frac{\Delta T_{12} k_g (2/\pi)\tan^{-1}\sqrt{x^2-1}\; x\,d\theta\,dx}{\delta_{Hz} + (n_i+1)ML + 2n_i(K-1)\delta_{i1}(x,\theta)} \tag{44}$$

where δ_{i1} and x_{i1} are given by Equations (30) and (31) respectively. Equation (44) reduces to the limiting case (integrand of Equation (36)) for $n_i=0$.

Equation (44) may be integrated in global coordinates, as was Equation (36). However, the resulting integral could not be reduced to the single integral, like Equation (37) because the integrand is dependent on θ through δ_{i1}. This complicates the evaluation of the integral because of the functional nature of θ_i, the upper limit of the θ integration.

The double integration in Equation (44) can be simplified by transforming the geometry to local coordinates, Figure 9. In this system, the integration limits are constants:

$$0 \le x_i \le L\epsilon_i \tag{45}$$

$$0 \le \theta_i \le \pi \tag{46}$$

so that

$$Q_{g2i} = \frac{2k_g\Delta T_{12}}{\pi} \int_0^{L\epsilon_i}\int_0^{\pi} \frac{x_i\tan^{-1}\sqrt{x^2-1}\; d\theta_i\,dx_i}{\delta_{Hz}(x) + (n_i+1)ML + 2n_i(K-1)\delta_i(x_i)} \tag{47}$$

$$Q_{g2i} = \frac{2k_g a\Delta T_{12}}{\pi} I_{g2i} \tag{47a}$$

where $\delta_{Hz}(x)$ and $\tan^{-1}\sqrt{x^2-1}$ retain the global coordinate x. The coordinate x is given by

$$x^2 = x_i^2 + x_{ci}^2 - 2x_i x_{ci}\cos\theta_i \tag{48}$$

and

$$\delta_i(x_i) = \sqrt{(L\epsilon_i)^2 - x_i^2} \tag{48a}$$

The local coordinate approach shortens computation time for the integral.

The resistance for the string of interstitial spheres is

$$\frac{1}{R'_{g2i}} = \frac{Q_{g2i}}{\Delta T_{12}} = \frac{2k_g a}{\pi} I_{g2i} \tag{49}$$

and $2N_i$ of these added in parallel gives the ith-ring contribution to the gap resistance:

$$\frac{1}{R_{g2i}} = 2k_o a\left[\frac{2N_i}{\pi} I_{g2i}\right] \tag{50}$$

where I_{g2i} is evaluated by adaptive numerical quadrature.

An alternative approach to calculating the interstitial sphere contribution is shown in Figure 12, in which the stack of spheres from plane m1 to m2 is replaced by the effective conductivity k_{te} as calculated by the basic-cell approach (Turyk, 1985). However, this is not the correct approach because the interstitial stack is not infinite, which is an underlying assumption in the basic-cell method. In the gap, the interstitial spheres transfer heat in a manner similar to that of a packed bed at a boundary wall (Peterson and Fletcher, 1988, Turyk, 1985). The formulation of the gap resistance is inconsistent as well, since substitution of $n_i=0$ does not reduce to the basic-cell formulation: a k_{te} term still remains in the equation. The calculation of the total cell conductivity would be overpredicted, and thus this approach is not recommended.

The total gap resistance R_g is calculated by adding the contributions of each of the m rings of stacked spheres in parallel with the basic-cell resistance, less the resistance of the interstitial-sphere regions with gas alone:

$$\frac{1}{R_g} = 2k_o aI + \sum_{i=1}^{m}\left[\frac{1}{R_{g2i}} - \frac{1}{R_{gli}}\right] \tag{51}$$

$$\frac{1}{R_g} = 2k_o a\left(I + (2/\pi)\sum_{i=1}^{m} N_i(I_{g2i} - I_{gli})\right) \tag{52}$$

The total cell effective thermal conductivity is calculated as for the basic model, resulting in

$$k_{te}^* = \frac{1}{L}\left[\frac{1}{K} + I + (2/\pi)\sum_{i=1}^{m} N_i(I_{g2i} - I_{gli})\right] \tag{53}$$

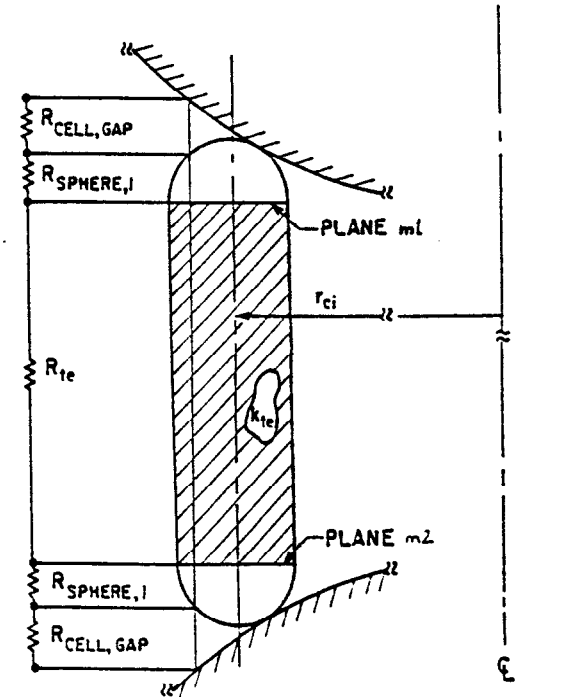

Figure 12 Alternative Method for Heat Transfer Through Interstitial Spheres

SAMPLE CALCULATION

A sample binary-component basic cell was formed and the effective thermal conductivity was evaluated to demonstrate the effect of the interstitial spheres. The sample calculation was carried out for interstitial spheres one-tenth the size of the primary component, ϵ_1=0.1, for two load values L=50 (heavy) and L=1000 (light), and for two gas-solid conductivity ratios K^{-1}=100 and K^{-1}=5000. The gas parameter M is varied from 10^{-6} (high pressure) to 10^{3} (vacuum). The features of the binary cell are illustrated in Figure 4, and the geometry is summarized in Table 1. The calculated results are tabulated in Tables 2 and 3, and illustrated in Figures 13 and 14, which also include values for the basic model (no interstitial spheres).

For the basic model, the effective conductivity of the cell increases with increasing gas pressure (lower M), increasing load (lower L) and increasing solid-to-gas conductivity ratio (lower K). As gas pressure decreases, there is no gas to conduct heat through the gap, so that the effective gap conductivity k_{se}^* approaches zero, and the cell total effective conductivity is controlled by heat conduction through the contact. The contact resistance decreases as load increases (contact radius increases) and as the conductivity of the solid phase increases; the cell effective conductivity becomes greater.

It is clear from Tables 2 and 3 that the interstitial spheres increase the effective gap and total conductivities. This is because of the increase in conducting strength of the interstitial gap medium. The greatest increases in the gap and total effective conductive conductivities occurs at high pressures (low M). At low pressures, little gas transmits heat from sphere to sphere, and because of point contact between the spheres of the secondary component, k_{se}^* approaches the no-interstitial-sphere value. The increase in the gap conductivity has the largest relative influence on the total effective conductivity in cases where L and K^{-1} are low.

The effective conductivity of the cell with interstitial spheres was not compared with experimental data found in the literature. Hall and Martin (1981), Ades and Peddicord (1982a), and Willison (1982) report some experimental measurements on the effective conductivity of binary and ternary beds of uranium-dioxide and uranium-carbide sphere-pac fuel. The experimental results in these papers cannot be compared directly with the numerical results in the previous section since the sphere size ratios are not comparable. However, the trends exhibited by the sample calculations here and the experimental data in Ades and Peddicord (1982a) and Willison (1982), with respect to addition of a secondary component, indicate that the present model is qualitatively correct.

To quantitatively assess the performance of the model compared with experimental data, a basic cell with ϵ_1=0.075 should be constructed, and the effective conductivity should be calculated over a range of gas pressures, and including appropriate thermophysical data for the experimental conditions in the literature. The load, and hence L, in the bed is difficult to assess, but a parametric study over a range of L compared with the experimental results may show which value is suitable. By comparing the calculations with experimental results, the strengths and shortcomings of the effective conductivity model can be determined, and work to further improve the model could be identified.

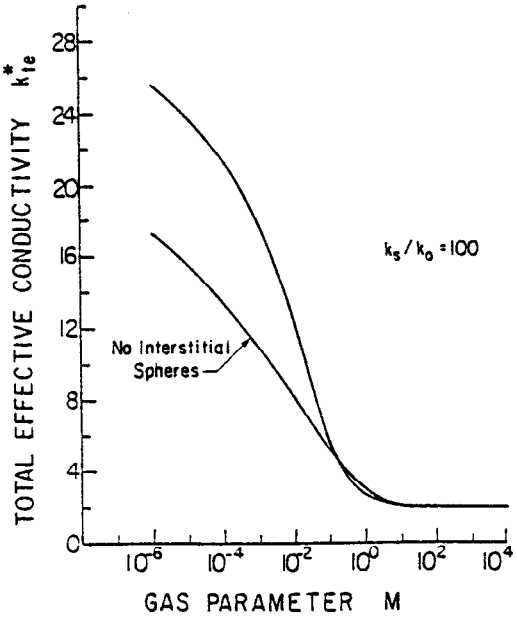

Figure 13a Total Effective Conductivity of Binary-Component Basic Cell for L=50 and K^{-1}=100

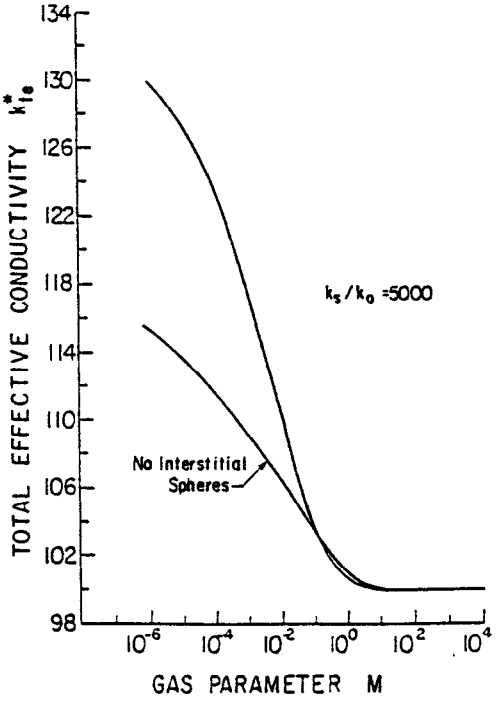

Figure 13b Total Effective Conductivity of Binary-Component Basic Cell for L=50 and K^{-1}=5000

DISCUSSION

The geometry of the packing of the interstitial spheres and the handling of the heat transfer analysis with the gap are admittedly simplistic compared with real binary-component packed beds. McGeary (1961) discussed realistic packing of multicomponent packed beds, and showed that while the larger component may be packed in a regular manner, the secondary component packs in a more complicated random fashion. In addition, Ades and Peddicord (1982b) wrote that multicomponent sphere-pac nuclear fuel becomes restructured (sintered) at elevated temperatures, thus changing the thermal conductivity of the system. However, the analysis presented is a first step towards making a deterministic analysis of binary-component packed bed heat transfer, while retaining the dependence of the conductivity on thermophysical properties.

In a more advanced analysis, the approach presented for the heat transfer analysis can be used for more complex packing of the interstitial spheres to account for the randomness of the secondary component, as long as the locations, size, and properties of the secondary component are known, or correlated. For example, a combination of numerical simulation, such as the Monte Carlo method of Yang et al. (1982) and the analytical basic-cell model could be used for real packed bed heat transfer.

The assumption of secondary-component point contact also simplified the analysis, and its effect should be addressed. Point contact led to the further assumptions that the temperature distribution on the surfaces of the large spheres was unaffected, that there was no contact conductance between the small and large spheres, and that heat flow was parallel to the axis of symmetry. In real packed beds, there is some small, finite area contact region between the large and small spheres, because the smaller spheres will carry some of the mechanical load. In this case, the local temperature field will change because of the presence of the contact. Further, the small spheres may still have some effect on the heat flow through the large spheres, even with the point contact assumption. The heat flow path is less resistive in the gap because of the increase in conductivity created by the small spheres. The gas in the gap would affect the temperature distribution in this manner also, but this was ignored in the basic model since it was argued that the effect would be small. The same argument may apply to the small spheres in the gap; it would be difficult to determine their effect on the temperature distribution, and the net effect may be small. Also, the small spheres are far enough away from the main contact so that the temperature drop does not vary much in the region of interest, i.e., the surfaces of the large spheres are nearly isothermal far from the contact.

Inclusion of these effects into the formulation of the binary-component basic-cell conductivity would be complex and highly dependent on the distribution of the spheres of the secondary phase. This may prove to be impractical for engineering work. A compromise solution would be to correlate the analytical model presented here with experimental data for various combinations of large and small spheres.

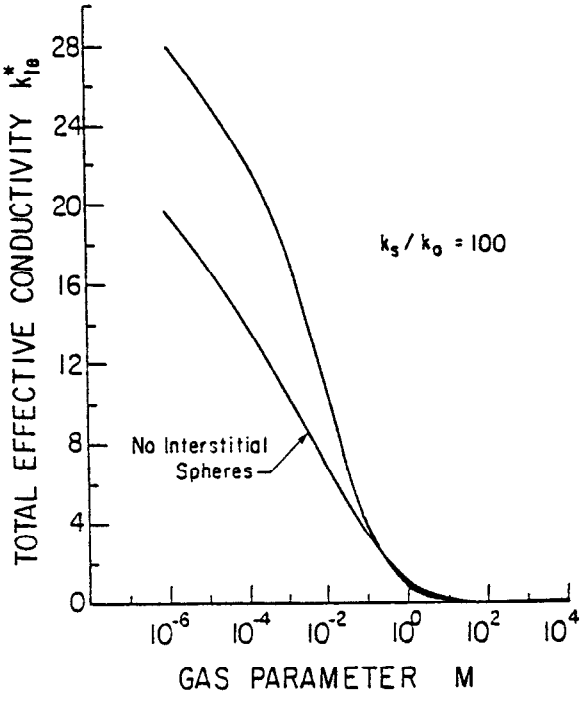

Figure 14a Total Effective Conductivity of Binary-Component Basic Cell for L=1000 and K^{-1}=100

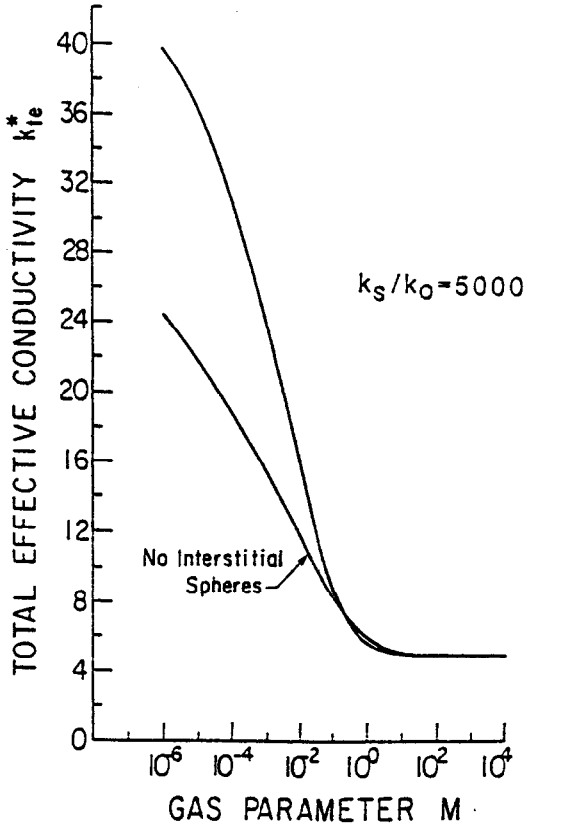

Figure 14b Total Effective Conductivity of Binary-Component Basic Cell for L=1000 and K^{-1}=5000

Table 1 Geometric Quantities in Binary-Component Basic Cell

Ring Number (i)	1		2		3	
Number of Interstitial Spheres (n_i)	1		2		4	
Load Parameter (L)	x_{c1}	N_1	x_{c2}	N_2	x_{c3}	N_3
50	22.9556	14	31.6508	19	42.4427	26
1000	458.2597	14	632.4570	19	848.5290	26

Table 2 Effective Conductivity of Binary-Component Basic Cell for L=50

M	K^{-1} = 100				K^{-1} = 5000			
	No Interstitial Spheres		w/Interstitial Spheres		No Interstitial Spheres		w/Interstitial Spheres	
	k_{ge}^*	k_{te}^*	k_{ge}^*	k_{te}^*	k_{ge}^*	k_{te}^*	k_{ge}^*	k_{te}^*
10^{-6}	15.3326	17.3326	23.6232	25.6232	15.3326	115.3326	29.8981	129.8981
10^{-5}	13.4706	15.4706	21.7445	23.7445	13.4706	113.4706	27.4195	127.4195
10^{-4}	11.4678	13.4678	19.5837	21.5837	11.4678	111.4678	23.1149	123.1149
10^{-3}	9.1277	11.1277	16.1447	18.1447	9.1277	109.1277	17.2477	117.2477
10^{-2}	6.3174	8.3174	10.0921	12.0921	6.3174	106.3174	10.2715	110.2715
10^{-1}	3.3060	5.3060	3.5655	5.5655	3.3060	103.3060	3.5771	103.5771
10^{0}	0.9880	2.9880	0.6744	2.6744	0.9880	100.9880	0.6746	100.6746
10^{1}	0.1437	2.1437	0.0865	2.0865	0.1437	100.1437	0.0865	100.0865
10^{2}	0.0152	2.0152	0.0090	2.0090	0.0152	100.0152	0.0090	100.0090
10^{3}	0.0015	2.0015	0.0009	2.0009	0.0015	100.0015	0.0009	100.0009

Table 3 Effective Conductivity of Binary-Component Basic Cell for L=1000

M	K^{-1} = 100				K^{-1} = 5000			
	No Interstitial Spheres		w/Interstitial Spheres		No Interstitial Spheres		w/Interstitial Spheres	
	k_{ge}^*	k_{te}^*	k_{ge}^*	k_{te}^*	k_{ge}^*	k_{te}^*	k_{ge}^*	k_{te}^*
10^{-6}	19.4782	19.5782	27.9878	28.0878	19.4782	24.4782	34.4554	39.4554
10^{-5}	16.8323	16.9323	25.3248	25.4248	16.8323	21.8323	31.1742	36.1742
10^{-4}	13.7024	13.8024	22.0321	22.1321	13.7024	18.7024	25.6723	30.6723
10^{-3}	10.2816	10.3816	17.4803	17.5803	10.2816	15.2816	18.6177	23.6177
10^{-2}	6.7721	6.8721	10.6385	10.7385	6.7721	11.7721	10.8225	15.8225
10^{-1}	3.4392	3.5392	3.7043	3.8043	3.4392	8.4392	3.7161	8.7161
10^{0}	1.0162	1.1162	0.6966	0.7966	1.0162	6.0162	0.6968	5.6968
10^{1}	0.1474	0.2474	0.0890	0.1890	0.1474	5.1474	0.0890	5.0890
10^{2}	0.0156	0.1156	0.0093	0.1093	0.0156	5.0156	0.0093	5.0093
10^{3}	0.0016	0.1016	0.0009	0.1009	0.0016	5.0016	0.0009	5.0009

CONCLUSIONS AND RECOMMENDATIONS

A simple method for the analysis of binary-component effective thermal conductivity was outlined. The model includes a simple packing of the interstitial spheres which greatly simplified the mathematical analysis. The method modified the conductivity of the basic model (no secondary component) by removing the contribution to the gap conductance of the gas alone and replacing it with the contribution of the interstitial spheres.

A sample calculation for a binary cell with one-tenth-sized interstitial spheres over a range of mechanical load, gas pressure, and solid-to-gas conductivity ratio was carried out. At low values of gas parameter (high pressure), the interstitial spheres increased the total effective conductivity of the basic cell. As with the single-component basic cell, at low gas pressures, the cell conductivity was controlled by the load and solid conductivity.

The calculated results agreed qualitatively with published experimental data. The method should be used to construct a basic-cell model for the types of beds reported in the literature, and calculations compared with the experimental results.

A deterministic model for the true packing of interstitial spheres, with interstitial sphere loading included may be impractical. A semi-empirical model using the method presented here may be a more appropriate approach.

ACKNOWLEDGEMENTS

The authors acknowledge the financial support of the Natural Sciences and Engineering Research Council of Canada in the forms of a Postgraduate Scholarship (PJT) and Grant A7445 (MMY). Mr. Turyk is also grateful to the National Research Council Canada for allowing him to publish this paper.

REFERENCES

Ades, M. J., and K. L. Peddicord, 1982a, "A Model for Effective Thermal Conductivity of Unrestructured Sphere-Pac Fuel", Nuclear Science and Engineering, v 81, p 540.

Ades, M. J., and K. L. Peddicord, 1982b, "Effective Thermal Conductivity of Sphere-Pac Fuel During Restructuring", Nuclear Science and Engineering, v 81, p 563.

Hall, R. O. A., and D. G. Martin, 1981, "The Thermal Conductivity of Powder Beds", Journal of Nuclear Materials, v 101, p 172.

Kitscha, W. W., and M. M. Yovanovich, 1975, "Experimental Investigation on the Overall Thermal Resistance of Sphere-Flat Contacts", in Heat Transfer with Thermal Control Applications, M. M. Yovanovich, (Ed.), Progress in Astronautics and Aeronautics, Vol. 39, AIAA, MIT Press, Cambridge MA.

McGeary, R. K., 1961, "Mechanical Packing of Spherical Particles", Journal of the American Ceramic Society, v 44, p 513.

Ogniewicz, Y., and M. M. Yovanovich, 1978, "Effective Conductivity of Regularly Packed Spheres: Basic Cell Model with Constriction", in Heat Transfer and Thermal Control Systems, L. S. Fletcher, (Ed.), Progress in Astronautics and Aeronautics, Vol. 60, AIAA, New York.

Peterson, G. P., and L. S. Fletcher, 1988, "Thermal Contact Conductance of Packed Beds in Contact with a Flat Surface", ASME Journal Heat Transfer, v 110, p 38.

Peterson, G. P., L. S. Fletcher, and K. L. Peddicord, 1988, "A Review of the Effective Thermal Conductivity in Multi-Fraction Reactor Fuels", in Proceedings of ASME/JSME Joint Thermal Engineering Conference, p 439, ASME.

Timoshenko, S., and G. N. Goodier, 1970, Theory of Elasticity, McGraw Hill, New York.

Turyk, P. J., 1985, "Modelling of Effective Heat Transfer Properties in Basic Cells of Binary Component Packed Beds with Interstitial Gas", M.A.Sc. Thesis, Dept. of Mech. Eng., Univ. of Waterloo, Canada.

Turyk, P. J., and M. M. Yovanovich, 1985, "Modified Effective Conductivity Models for Basic Cells of Simple Cubic Packed Beds", in Heat Transfer in Porous Media and Particulate Flows, L. S. Yao, et al., (Eds.), ASME HTD-Vol. 46.

Willison, J. S., 1982, "Thermal Conductivity Modelling of Unstructured Sphere Pac Nuclear Fuels", M.Sc. Thesis, Oregon St. U.

Yang, Y. S., J. R. Howell, and D. E. Klein, 1982, "Monte Carlo Simulation of Thermal Conduction Through a Randomly Packed Bed of Spheres", in Heat Transfer 82, Proceedings of the Seventh International Heat Transfer Conference, p 109, Hemisphere Publ. Corp., Washington.

Yovanovich, M. M., 1967, "Thermal Contact Resistance Across Elastically Deformed Spheres", Journal of Spacecraft and Rockets, v 4, p 119.